The Journal of Experimental Biology 213, 1195-1206

doi:10.1242/jeb.034330

The scaling of myofibrillar actomyosin ATPase activity in apid bee flight muscle in relation to hovering flight energetics

Graham N. Askew[1,*], Richard T. Tregear[2] and Charles P. Ellington[3]

[1]Institute of Integrative and Comparative Biology, University of Leeds, Leeds, UK, [2]MRC Laboratory of Molecular Biology, Hills Road, Cambridge, UK and [3]Department of Zoology, Downing Street, University of Cambridge, Cambridge, UK

*Author for correspondence (g.n.askew@leeds.ac.uk)

Accepted 14 December 2009

SUMMARY

For all types of locomotion, the overall efficiency with which chemical energy is converted into mechanical work increases with increasing body size. In order to gain insight into the determinants of the scaling of overall efficiency, we measured the scaling of the rate of ATP utilisation during cyclical contractions using glycerinated fibres from the dorsolongitudinal flight muscle of several species of apid bees, covering a ninefold range in body mass. The efficiency of ATP utilisation by the crossbridges is one of the stages that determines the overall efficiency of locomotion. The mechanochemical coefficient was calculated from the ratio of the net power output to the rate of ATP hydrolysis and ranged from 6.5 to 9.7 kJ mol^{-1} ATP. The corresponding gross myofibrillar efficiency was 15–23%, increasing concomitantly with body mass (M_b) and decreasing with increasing wingbeat frequency (n) and scaling as $M_b^{0.184}$ and $n^{-1.168}$ in bumblebees and as $M_b^{0.153}$ and $n^{-0.482}$ in euglossine bees. Overall efficiency of hovering in bumblebees and euglossine bees was calculated using previously published metabolic power data and revised estimates of the mechanical power output to take into account the drag due to the leading edge vortex that has not been included in previous models. The scaling of overall efficiency of hovering flight in apid bees was not as pronounced as the scaling of myofibrillar efficiency. Therefore the scaling of myofibrillar efficiency with body mass (or frequency) only explained part of the scaling of overall efficiency, and it is likely that the efficiency of other steps in the transduction of chemical energy into mechanical work (e.g. the efficiency of mitochondrial oxidative recovery) may also scale with body mass.

Key words: myofibrillar ATPase, scaling, efficiency, insect flight muscle.

INTRODUCTION

Based on the metabolic cost and mechanical requirements of locomotion, it seems that for all types of locomotion overall efficiency increases with increasing body size (Alexander, 2005). Whole animal metabolic rate represents a summary of all of the metabolic processes that occur during locomotion. In order to explain the observed scaling of locomotor energetics we need to be able to partition the energy costs between different metabolic processes. A major source of energy expenditure is the muscles that drive locomotion. For example, during terrestrial locomotion, the hindlimb muscles use over 80% of the total metabolic energy (Ellerby et al., 2005). Active muscles use energy during crossbridge cycling, when metabolic energy is converted into mechanical work. The amount of metabolic energy consumed relative to the crossbridge work performed is determined by the efficiency of this conversion. The 'overall efficiency' with which metabolic energy is transferred into mechanical work is determined by the efficiency of a number of underlying steps. (1) The performance of mechanical work by the actomyosin interaction during the crossbridge cycle, utilizing chemical energy derived from the hydrolysis of ATP. This determines the 'myofibrillar efficiency' or cross-bridge thermodynamic efficiency (Smith et al., 2005). (2) The regeneration of high-energy phosphates (e.g. ATP and PCr) by mitochondrial oxidation phosphorylation. This determines the 'oxidative recovery efficiency'. (3) The transfer of work performed by the crossbridges to the environment, either by the application of a force or by the performance of mechanical work. At each stage within this process, energy may be lost through the inefficient transfer of energy from one step to the next. In addition, there may be energy costs associated with processes that are required to sustain the contraction but that do not directly contribute to the mechanical output of the muscle (e.g. Ca^{2+} cycling in some muscles). The overall efficiency with which chemical energy is converted into mechanical work is a major factor in determining the metabolic cost of locomotion.

Variation in muscle efficiency with speed of contraction

It is likely that differences in crossbridge cycling rate are far more important determinants of efficiency than is body mass, and that the scaling of overall efficiency with body mass is associated with the concomitant decrease of contraction frequencies with increasing size. Muscle efficiency measurements have been made for both fast and slow muscles from a small number of animals from both whole muscles and from individual fibres of known molecular composition. These experiments have been performed during both isovelocity and cyclical contractions. Under isovelocity conditions, some experiments have revealed no significant difference in the initial efficiency between fast and slow muscles from mice (Barclay et al., 1993), or in the myofibrillar efficiency between single skinned fibres from humans with different myosin isoform composition (He et al., 2000). However, other experiments, for example on mammalian and amphibian limb muscles, have shown the initial or myofibrillar efficiency of slow muscles to be higher than in fast muscles during isovelocity contractions (Barclay, 1996; Buschman et al., 1996; Buschman et al., 1997; Reggiani et al., 1997). During sinusoidal contractions, which simulate more accurately than isovelocity contractions the way in which many muscles perform during

locomotion (in particular during flight), it has been found in muscles from dogfish (Curtin and Woledge, 1993a; Curtin and Woledge, 1993b) and mice (Barclay, 1994) that fast muscles have a lower initial efficiency than slow muscles, although this difference disappears when comparing the net efficiency of fast and slow muscles, indicating that there are differences in the efficiency of mitochondrial oxidative metabolism (Barclay and Weber, 2004). These results are highly relevant to the scaling relationships derived from locomotion studies. Smaller animals need faster muscles because of their higher locomotor frequencies, and their lower overall efficiency is consistent with the results for fast and slow muscles. However, while there are data to suggest that intraspecifically fast muscles are less efficient than slow muscles, there are insufficient data to enable the interspecific scaling of efficiency to be determined. Differences in the efficiency between fast and slow muscles are likely to be due to the different operating frequencies.

Although a number of studies have determined the allometric scaling of overall efficiency, there is very little information available about whether or how either the mitochondrial oxidative recovery or myofibrillar efficiencies vary in different sized organisms. In order to separate the factors that determine the scaling of overall muscle efficiency, the scaling must be determined for each of the processes that contribute to the conversion of chemical energy into mechanical work: the activation costs associated with calcium cycling, the crossbridge efficiency, and the mitochondrial oxidative recovery efficiency. A model system in which the determinants of overall efficiency can be separated is the glycerinated asynchronous insect flight muscle preparation. Use of glycerinated *asynchronous* insect flight muscle has a number of advantages over skeletal muscle because of the unique way in which this muscle is activated. First, the complication of ATP usage by sarcoplasmic reticulum Ca^{2+} pumps is eliminated because Ca^{2+} release is asynchronous with and at a lower rate than that of the muscle contractions. A second advantage is that the manner in which asynchronous insect flight muscle is stretch activated and deactivated by shortening means that glycerinated muscle fibres can be studied during cyclical contractions that mimic *in vivo* performance, rather than during isovelocity contractions (e.g. Jewell and Rüegg, 1966; Pringle and Tregear, 1969; Gilmour and Ellington, 1993). Third, glycerination of the muscle fibres leaves only the contractile proteins and connective tissue intact, allowing the myofibrillar actomyosin ATPase activity to be studied in isolation of all other processes. The scaling of the mitochondrial oxidative recovery efficiency can then be inferred from the scaling of overall and myofibrillar efficiencies. Fourth, the overall efficiency of insect flight can be determined using respirometry and aerodynamic calculations (see below). This allows the scaling of myofibrillar efficiency to be considered in relation to the whole animal locomotor efficiency.

Energetics of hovering and the scaling of overall efficiency in apid bees

The extreme manoeuvrability and ability to fly in confined spaces of many insects makes them ideal subjects for studies of hovering energetics using respirometry (e.g. Casey and Ellington, 1989; Cooper, 1993; Dickinson and Lighton, 1995; Borrell and Medeiros, 2004; Darveau et al., 2005; Suarez et al., 2005). In conjunction with metabolic measurements, recordings of wing kinematics and morphological measurements can be used to carry out a detailed aerodynamic analysis to estimate the mechanical power requirements of the flight muscles and hence to determine the allometric scaling of the metabolic and mechanical power requirements of hovering [e.g. interspecifically for several species of euglossine bees (Casey and Ellington, 1989) and intraspecifically for worker and queen bumblebees (Cooper, 1993)]. The ratio of the mechanical power output to the metabolic power requirements gives the overall efficiency of hovering. In euglossine bees and bumblebees the overall efficiency of hovering increases with increasing body mass (Casey and Ellington, 1989; Cooper, 1993).

It has come to light that previous studies may have underestimated the mechanical power requirements of flight (Ellington, 1999; Sane and Dickinson, 2001). Quasi-steady analyses have failed to account for the presence of the leading edge vortex (LEV) (Ellington et al., 1996) that appears to be a general feature of insect flight and, as a result, have underestimated the mean drag coefficient. Recent measurements using dynamically scaled mechanical insect models have confirmed that the profile drag ($C_{D,pro}$), due to the skin friction and form drag on the wings has been underestimated (Sane and Dickinson, 2001). The effect of not taking account of the LEV is that previous analyses have underestimated the profile power component of flight and, as a result, have underestimated both the total mechanical power requirements and overall efficiency for hovering. However, it is not yet know how the scaling relationship of overall efficiency with body mass will be affected.

In this study we determined the scaling of myofibrillar efficiency of glycerinated muscle fibres taken from the dorsal-longitudinal flight muscles of euglossine bees and bumblebees. We also performed an aerodynamic analysis (taking into account the increased drag due to the LEV) on previously published data to determine the mechanical power requirements of hovering in bees and the scaling of overall hovering efficiency. Comparison with re-analysed data for the scaling of the overall efficiency in the same species, enabled us to determine the extent to which the scaling of overall efficiency is determined by the scaling of myofibrillar efficiency. This is the first attempt to link the scaling of overall locomotor efficiency with the efficiency of the actomyosin interaction.

MATERIALS AND METHODS

Measurement of myofibrillar efficiency

Animals

Five species of euglossine bees (*Eulaema meriana* Olivier 1789, *Exaerete frontalis* Guérin-Méneville 1844, *Eulaema nigrita* Lepeletier 1841, *Euglossa imperialis* Cockerell 1922 and *Euglossa bursigera* Moure 1970) were collected on Barro Colorado Island (Republic of Panama) under licence during March 2000. Male bees were attracted using baits impregnated with 1,8-cineole positioned approximately 1–2.5 m from the ground (Roubik and Ackerman, 1987). The insects were stored in collecting vessels for no more than 2 h prior to dissection.

Bumblebees (*Bombus terrestris* Linnaeus 1758) were raised from colonies (Koppert UK Ltd, Haverhill, Suffolk, UK) kept in Natupol hives housed in a laboratory (temperature approximately 18°C). The bees were fed a solution containing equal volumes of honey and tap water and given access to pollen. The pollen was located within a flight chamber and it was necessary for the bees to fly in order to access it in an attempt to maintain the animals' flight fitness.

Dissection of the dorsal-longitudinal muscles

All of the experiments were carried out using the dorsal-longitudinal muscles (DLM). These muscles were selected as they are the largest flight muscles, comprising long parallel fibres. The insect was immobilised by placing it in a plastic container surrounded by ice for approximately 10 min. The head, legs, wings (leaving the wing bases intact for orientation) and, in bumblebees, sting were removed.

The abdomen was carefully removed from the thorax, at the same time withdrawing the gut from the thorax and taking great care not to rupture it. Immediately, the thorax was rinsed with cold, buffered saline to remove any protease enzymes that might have spilled from the gut. The DLM was exposed by taking a sagittal section through the thorax.

Glycerination procedure

The glycerination procedure for these bee muscles followed methods developed for the glycerination of the DLM from the waterbug *Lethocerus* (M. K. Reedy, personal communication). The solutions used for the glycerination and storage of the DLM had the following composition: 20 mmol l^{-1} phosphate buffer (pH set to 6.8 at 18°C), 5 mmol l^{-1} potassium EGTA, 5 mmol l^{-1} sodium azide, 10 mmol l^{-1} potassium chloride, 2 mmol l^{-1} magnesium chloride, 5 mmol l^{-1} magnesium ATP. The procedure for glycerol extraction of the fibres involved gradually increasing the concentration of glycerol within the solution from zero to 75% by volume. Triton X-100 (1%) was used to chemically permeablise the muscle, removing all of the membranes and leaving only the contractile proteins and connective tissues intact. Sodium azide was used to inhibit mitochondrial ATPase activity. Protease inhibitors [0.5 mmol l^{-1} phenylmethylsulphonyl fluoride (PMSF) and half Complete™ mini, EDTA-free protease inhibitor tablet (Boehringer Mannheim) per 5 ml were used in the initial stages of extraction to prevent damage to the contractile proteins. Glycerinated fibres were stored at –80°C for up to 9 months before the mechanical and/or energetics experiments presented here were carried out. The storage solution contained 0.1 mmol l^{-1} dithiothreitol and half Complete™ mini, EDTA-free protease inhibitor tablet (Boehringer Mannheim) per 5 ml.

Mechanical power output of glycerinated myofibrils

The net mechanical power output of the glycerinated muscle fibres was determined using the work loop technique (Machin and Pringle, 1959; Josephson, 1985). In the work loop technique the muscle is subjected to cyclical length changes at a cycle frequency appropriate to its normal activity pattern. Asynchronous muscle performs oscillatory contractions when activated without the need for electrical stimulation in each cycle (Josephson et al., 2000b). A plot of muscle force against length traces a loop, the area of which is the net work per cycle; power output is net work multiplied by cycle frequency.

Frozen, glycerinated fibres were allowed to warm up to room temperature (approximately 18°C), and single fibres carefully teased away from the muscle. The fibres were pared down to a diameter of approximately 50–100 μm. The fibres were mounted on to the mechanical apparatus between a force transducer (SensoNor AE801, Horten, Norway) and a mechanical vibrator (Ling Dynamic Systems V101, Royston, Herts, UK) using glue made from cellulose nitrate dissolved in acetone. Further details of the work loop apparatus have been published previously (Gilmour and Ellington, 1993). The length of the muscle was controlled using a computer-generated wave in the application Testpoint (version 3.0; Capital Equipment Corporation, Billerica, MA, USA) and converted into an analogue signal by a 12-bit D/A converter. Force and length were amplified and recorded on a personal computer using a 12-bit A/D converter and a sampling frequency of 10 kHz (DAS1802AO, Keithley Instruments, Theale, UK).

Experiments were carried out in a solution comprising a mixture of activating solution (20 mmol l^{-1} Pipes buffer pH 7.0 at 18 °C, 5 mmol l^{-1} calcium EGTA, 5 mmol l^{-1} sodium azide, 2 mmol l^{-1} magnesium chloride, 10 mmol l^{-1} magnesium ATP) and relaxing solution (20 mmol l^{-1} Pipes buffer pH 7.0 at 18°C, 5 mmol l^{-1} potassium EGTA, 5 mmol l^{-1} sodium azide, 10 mmol l^{-1} sodium chloride, 2 mmol l^{-1} magnesium chloride, 10 mmol l^{-1} magnesium ATP), with approximately 8 mmol l^{-1} phosphoenolpyruvate (PEP), 1.7 units pyruvate kinase (PK) and 3.1 units lactate dehydrogenase (LDH). For each insect carcass, a series of preliminary experiments were carried out in which the Ca^{2+} concentration ($[Ca^{2+}]$) was varied by mixing activating and relaxing solutions in different proportions. The $[Ca^{2+}]$ that yielded the highest net work at a particular cycle frequency was selected for all subsequent experiments. All experiments were carried out in a temperature controlled chamber at 25°C.

For each muscle, a series of preliminary experiments were carried out to determine the optimal strain over a range of cycle frequencies (Josephson et al., 2000b). The parameters that were varied were the mean length about which the muscle was oscillated [ε_0; referred to as extension in Gilmour and Ellington (Gilmour and Ellington, 1993)] and the strain [ε; referred to as peak-to-peak oscillatory strain in Gilmour and Ellington (Gilmour and Ellington, 1993)]. For each new starting length, the muscle was cycled over a range of strains that were varied every fifth cycle (Fig. 1A). Net power output was calculated as the average over cycles 2–4 for each set of loops. The force at each starting length and for each strain for a typical muscle are shown in Fig. 1, together with representative work loops. The strain determined to be optimal for maximising the net power output at each cycle frequency was used in the subsequent experiments to determine myofibrillar ATP utilisation (see below).

Measurement of myofibrillar ATP utilisation

The rate of ATP hydrolysis was determined in glycerinated muscle fibres by a NADH-linked assay (Loxdale, 1976; Glyn and Sleep, 1985; Stienen et al., 1996; Potma and Stienen, 1996; Reggiani et al., 1997; Syme et al., 1997; Rome and Klimov, 2000) in which resynthesis of ATP utilised by the muscle fibre (Eqn 1) was coupled to the oxidation of NADH. In this assay, ADP is rephosphorylated by PEP, catalysed by PK (Eqn 2). This reaction is coupled to NADH oxidation to NAD^+ and the reduction of pyruvate to L-lactate, catalysed by LDH (Eqn 3):

$$\mathrm{ATP} \rightarrow \mathrm{ADP} + \mathrm{P_i} \quad (1)$$

$$\mathrm{Phosphoenolpyruvate} + \mathrm{ADP} \rightarrow \mathrm{pyruvate} + \mathrm{ATP} \quad (2)$$

$$\mathrm{Pyruvate} + \mathrm{NADH} + \mathrm{H^+} \rightarrow \mathrm{lactate} + \mathrm{NAD^+}. \quad (3)$$

NADH absorbs light at a wavelength of 340 nm but NAD^+ does not, enabling the rate of ATP hydrolysis to be measured from the absorbance at 340 nm of the solution in which the fibre is bathed. The amount of NADH (q; in nmoles) in the solution was calculated using the Beer–Lambert law as follows:

$$q = \frac{v}{El}\log\left(\frac{I_t R_0}{R_t I_0}\right), \quad (4)$$

where v is the volume of solution in the chamber, E is the extinction coefficient for NADH at 340 nm (6.22×10^{-3} mol l^{-1} cm^{-1}), l is the path length, I_t is the intensity of the 340 nm beam at time t, R_t is the intensity of the reference beam at time t, I_0 is the intensity of the 340 nm beam with no NADH present, R_0 is the intensity of the reference beam with no NADH present. This approach was confirmed by the injection of known amounts of ADP into the chamber (see also Loxdale, 1976; Glyn and Sleep, 1985; Stienen et al., 1996; Potma and Stienen, 1996; Reggiani et al., 1997; Syme et al., 1997).

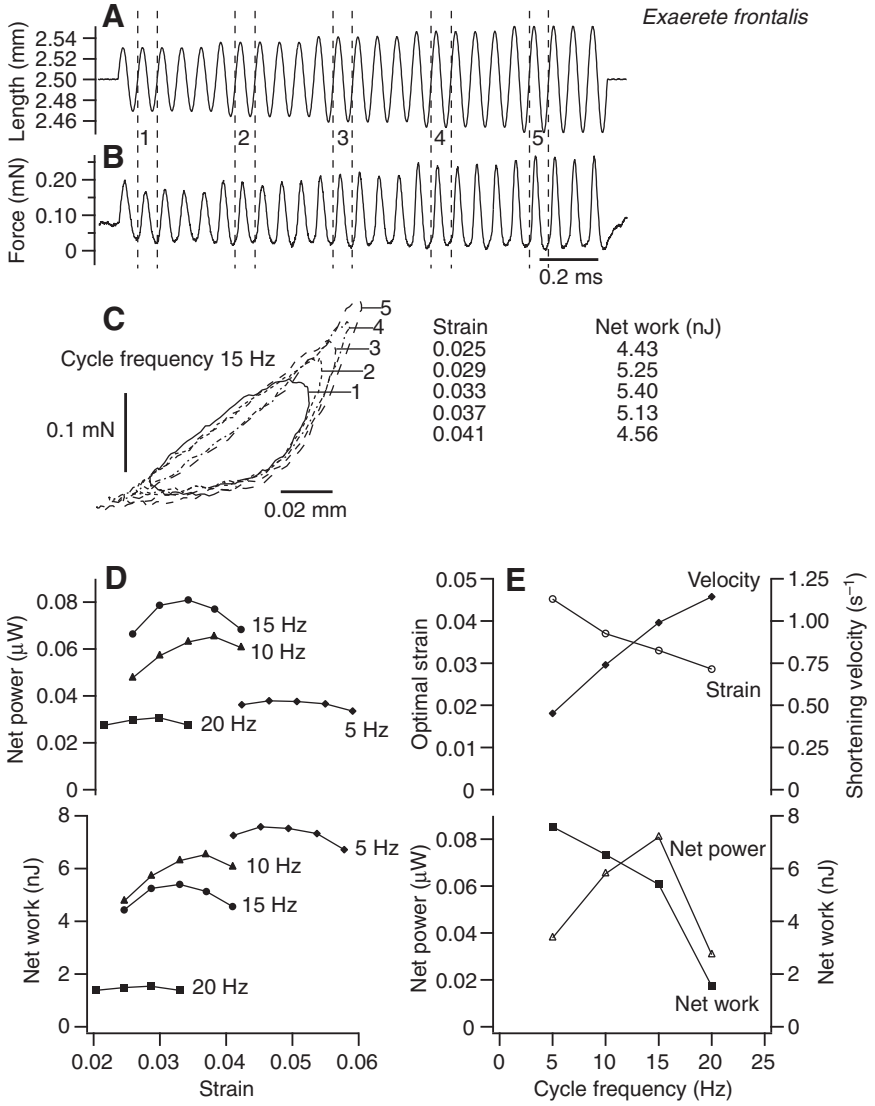

Fig. 1. Establishing the optimum working conditions for glycerinated, asynchronous bee flight muscle fibres. The muscle was subjected to a series of sinusoidal length changes at a constant cycle frequency. Every fifth cycle, the strain was increased so that within an oscillation series, the fibre was subjected to a range of strains. (A) The length of the muscle and (B) the force generated for fibre from *Exaerete frontalis* at an oscillation frequency of 15 Hz at 25°C.(C) Example work loops for each of the strains, with the relevant cycles numbered on the length and force records. (D) The effects of strain and cycle frequency on the net work and net power output from the fibre. At each cycle frequency there was a distinct optimum strain at which work and power output were maximal. (E) Optimal strain decreased with increasing cycle frequency, however, the average shortening velocity was not constant. Work decreased with increasing cycle frequency, but power output was maximal at an intermediate frequency.

The apparatus that was used to measure myofibrillar ATP consumption (Fig. 2) consisted of a temperature-controlled chamber into which the fibre could be sequentially immersed. The chamber was constructed from anodised aluminium and had a volume of approximately 100 μl. It had UV-fused silica glass windows (Comar Instruments, Cambridge, UK) that allowed transmission of light between 170–2500 nm. The path-length through the chamber was 5.4 mm. A well, hollowed out in the base of the chamber, acted as a guide for a stir bar. The temperature of the solution within the chamber was controlled to 25±0.3°C using a series of Peltier effect heat pumps and a precision temperature sensor in a feedback circuit.

Light from a 75 W xenon arc lamp was restricted in diameter and focused at the centre of the photometric chamber using a series of diaphragms and lenses. The light leaving the chamber was split using a dichroic beamsplitter into two beams, a reflected beam with a wavelength of 340–390 nm and a transmitted beam in the visible region. Bandpass interference filters were used to restrict each of these two beams to wavelengths of 340 nm and 435.8 nm, respectively. The 435.8 nm beam acted as a reference that enabled us to correct for fluctuations in the intensity of the beam entering the chamber and reduced stirring artefacts. The intensity of the beams of light was detected using UV enhanced 100 mm^2 photodiodes. The outputs were amplified, filtered and recorded at a sample frequency of between 100–500 Hz on a data acquisition board (DAS801, Keithley Instruments, Theale, UK) running in a personal computer.

Myofibrillar ATP consumption was measured over a range of cycle frequencies for each muscle fibre. The muscle was cycled for a period of 1–3 min at a particular cycle frequency at the optimal strain for that frequency. In the first few seconds of oscillation, the mean length was adjusted to that at which net work was maximal. In some case further minor adjustments of length were required to sustain the level of work.

The ratio of the net power output to the rate of ATP hydrolysis was calculated, and was termed the *mechanochemical coefficient* (MC; kJ mol^{-1}). The slope of the regression through the concentration of NADH (calculated using Eqn 4) with respect to time was used to determine the rate of ATP utilisation by the working fibre. The rate of ATP utilisation during the phase of oscillatory work was used to calculate the gross myofibrillar efficiency. Gross efficiency was calculated from the ratio of the total net mechanical work to the total metabolic energy expenditure and does not therefore include any deduction of resting metabolic rate (Josephson et al., 2001). In some of the previously published work on energy usage by glycerinated insect asynchronous flight muscles, the rate of ATP utilised during

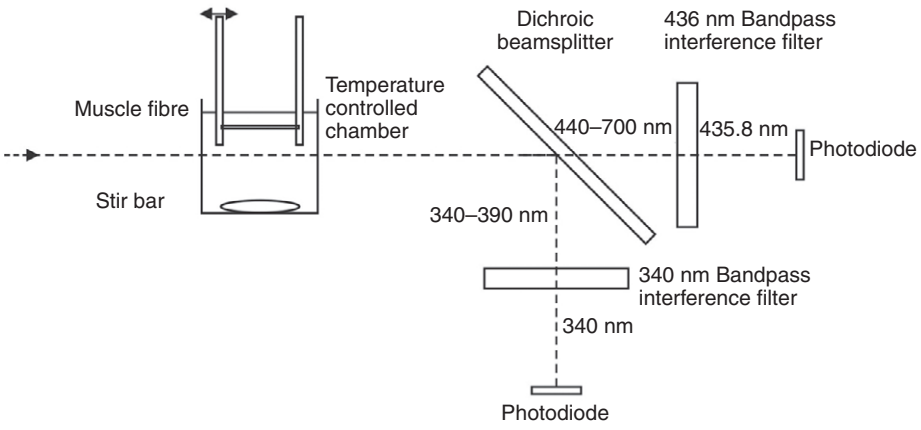

Fig. 2. Diagram of the experimental setup. A glycerinated muscle fibre was attached to a force transducer and a mechanical vibrator, and held in activating solution in a temperature-controlled chamber. The rate of ATP utilisation was determined photometrically by the enzymatic coupling of ATP utilisation to NADH oxidation. Light passing through the chamber was separated into UV and visible wavelengths using a 45° dichroic beamsplitter. Interference filters were used to isolate wavelengths of 340 nm and 435.8 nm. The intensity of the 340 nm beam was determined using a UV-enhanced photodiode and used to determine the concentration of NADH. The intensity of the 435.8 mn beam was used to correct for fluctuations in light intensity. A stir bar in the temperature-controlled chamber ensured adequate mixing of the activating solution.

the initial isometric phase has been subtracted from the rate of ATP consumption during cycling, giving a measure of what has been termed 'extra ATPase' (e.g. Rüegg and Tregear, 1966; Rüegg and Stumpf, 1969). To enable comparison with this previous work, the MC was also calculated as the ratio of power output to this extra ATPase (Steiger and Rüegg, 1969) and used to calculate the apparent efficiency. Apparent efficiency was calculated as the ratio of total net mechanical work to the metabolic energy associated with muscle contraction [i.e. total metabolic energy expenditure minus energy expended under similar conditions but with no work output (Josephson et al., 2001)]. The myofibrillar efficiency (gross or apparent; expressed as a percentage) was calculated as the ratio of MC to the free energy of hydrolysis of ATP. We established that the ends of the fibre encased in glue had no detectable ATP consumption and that there was no detectable ATP consumption in the absence of a fibre.

Revised estimates for the mechanical power requirements of hovering and calculation of overall efficiency

The calculation of the mechanical power requirements of hovering in bumblebees and euglossine bees were revised (using the same kinematic and morphological data) from previously published values (Cooper, 1993; Casey and Ellington, 1989) to take into account the increased drag due to the presence of the leading edge vortex that has subsequently been discovered (Ellington et al., 1996). The revised calculation of profile drag followed the suggestion that the lift to profile drag ratio was 1.7 (Ellington, 1999). Other than the revised estimate of $C_{D,pro}$, the calculation of the mechanical power requirements of hovering followed Ellington (Ellington, 1984). The overall efficiency of hovering was calculated as the ratio of the revised calculation of mechanical power output to the metabolic power input determined from previous studies (Cooper, 1993; Casey and Ellington, 1989).

Statistical analyses

Scaling relationships between variables were determined by plotting data on logarithmic axes and fitting a power curve to the data using the curve fitting routines in Igor Pro version 5 (Wavemetrics, Portland, Oregon, USA). Correlation coefficients (r) and P values were computed, indicating whether the scaling exponent was significantly different from zero. Where appropriate, the slopes and elevations of linear regression equations were compared using the Student's t-test (Zar, 1996).

RESULTS

Insect morphology and kinematics

The body masses of the euglossine bees covered an approximately ninefold size range, from 94 mg to 873 mg. There was a threefold body mass range between worker and queen bumblebees. The wingbeat frequency of the insects was not measured, but was calculated from published scaling equations [euglossine bees (Casey and Ellington, 1989) bumblebees (Cooper, 1993)]. Larger insects have a lower wingbeat frequency than small individuals. Within the euglossine bees there was a predicted twofold frequency range. Worker bumblebees had calculated wingbeat frequencies that were 21% more rapid than queen bumblebees.

Establishment of optimum working conditions: effects of strain and cycle frequency on power and work generation

For each species of insect, preliminary experiments were carried out to establish the optimum strain for a range of cycle frequencies over which the fibre could generate positive work. The net work performed by the muscle at each strain was determined for a range of cycle frequencies. For each cycle frequency, there was a distinct optimum strain at which the work generated and power output were maximal (Fig. 1D). The net work performed by the fibre decreased with increasing cycle frequency whereas net power output was maximal at an intermediate cycle frequency (Fig. 1E). Optimum strain decreased monotonically with increasing frequency (Fig. 1E). However, as has been observed in beetle muscle, the decrease in strain was insufficient to maintain a constant average shortening velocity (Josephson et al., 2000b). As a result, average shortening velocity increased with increasing cycle frequency (Fig. 1E).

Measurement of ATP utilisation

Fig. 3 shows data from a typical experiment, illustrating the approach that was used to measure the actomyosin ATPase during cyclical contractions. The intensity of the 435.8 nm beam showed minimal change during the course of the experiment. By contrast, the intensity of the 340 nm beam increased as the concentration of

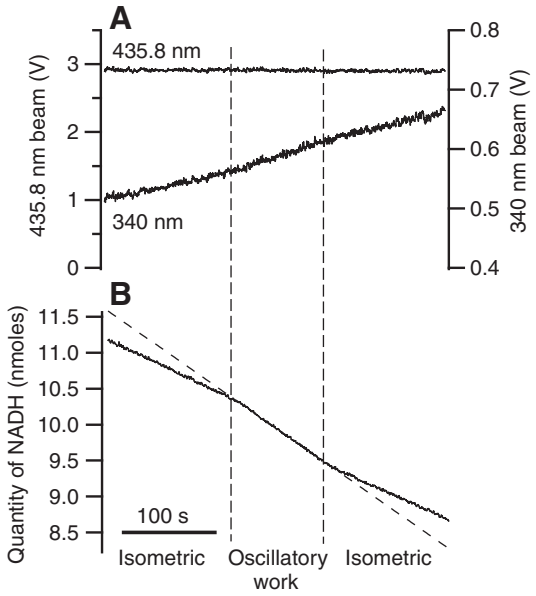

Fig. 3. Measurement of the rate of ATP utilisation in a glycerinated, asynchronous bee flight muscle fibre. (A) Intensity of 435.8 nm and 340 nm beams passing through the solution in which the fibre was held. ATP resynthesis was enzymatically coupled to the oxidation of NADH, so the intensity of the 340 nm beam, which is absorbed by NADH, increased as the fibre used ATP. (B) The quantity of NADH in the solution calculated using the Beer–Lambert law. The rate of ATP utilisation was calculated from the rate at which NADH was oxidised (indicated by a broken line). Initially the muscle was held isometrically, followed by a period of oscillatory work and a second isometric period (separated by vertical dashed lines).

NADH decreased. This resulted from NADH oxidation during the resynthesis of the ATP (Eqns 2 and 3) utilised by the fibre (Fig. 3A). The muscle fibre was held in activating solution throughout the experiment and consumed ATP both during the phase when the muscle fibre performed oscillatory work and in the phases when the muscle was held isometrically (before and after the oscillation). The rate of ATP utilisation of fibres performing positive work during oscillatory contractions was greater than fibres producing force under isometric conditions (Fig. 3B).

Effects of cycle frequency on power output and ATP utilisation

Glycerinated asynchronous flight muscle from euglossine bees and bumblebees when held in activating solution, stretched and subjected to oscillatory contractions, performed net positive work as has been previously observed (e.g. Rüegg and Tregear, 1966; Gilmour and Ellington, 1993). This work could be sustained continuously for several minutes. For each species of insect, there was an optimum cycle frequency at which power output was maximal (Fig. 1E, Fig. 4A–C). This is typical of both live (Josephson, 1997; Josephson et al., 2000b) and glycerinated muscle fibres (Jewell and Rüegg, 1966; Pybus and Tregear, 1975; Gilmour and Ellington, 1993) and is a general feature of all muscles (Altringham and Johnston, 1990; Askew and Marsh, 1997). Such an optimum exists because of the decrease in work with increasing cycle frequency.

The mechanochemical coefficient (MC) is a measure of the mechanical energy output per mole of ATP hydrolysed. As with the power output, MC was also highest at an optimum cycle frequency that was intermediate relative to the range of frequencies over which the muscle could generate net positive work (Fig. 4D–F). The optimum cycle frequency for maximum MC was similar to that which yielded the highest net power output (Fig. 4A–F).

For each species of insect, there was a wide range in the absolute net power output measured, because of variation in preparation size, variation with cycle frequency and variation in performance at each cycle frequency (Fig. 4G–I). However, for all species there was a highly significant (P<0.002) relationship between MC and power output, with MC increasing monotonically with power output (Fig. 4G–I). Thus fibres that generated high power outputs also had the highest MC.

Effects of body size and wingbeat frequency on mechanochemical coefficient and myofibrillar efficiency

The maximum average MC ranged from 6.5±0.5 kJ mol^{-1} (N=6) in *E. imperialis* to 9.7±0.4 kJ mol^{-1} in *E. frontalis* (N=6). In order to estimate the myofibrillar efficiency, the free energy of ATP hydrolysis (ΔG_{ATP}) was assumed to be 48 kJ mol^{-1} [appropriate for contracting muscle (Barclay, 1998; Kushmerick and Davies, 1969)]. Both gross and apparent myofibrillar efficiency increased with increasing body mass in both euglossine bees and in bumblebees (apparent efficiency: bumblebees $\propto M_b^{0.12}$ P<0.01, euglossine bees $\propto M_b^{0.24}$ P<0.01; gross efficiency: bumblebees $\propto M_b^{0.18}$ P<0.01, euglossine bees $\propto M_b^{0.16}$ P<0.01; Fig. 5A). The negative scaling of wingbeat frequency with body mass resulted in a significant decrease in both gross and apparent myofibrillar efficiency with increasing wingbeat frequency for the combined bee group (apparent efficiency $\propto n^{-0.75}$ in bumblebees P<0.01, $\propto n^{-0.80}$ in euglossine bees P<0.01; gross efficiency $\propto n^{-1.17}$ in bumblebees P<0.01, $\propto n^{-0.51}$ in euglossine bees P<0.01; Fig. 5B, Table 1).

Revised estimates of mechanical power requirements and overall efficiency of hovering

For mechanical power calculated using the original calculations, overall efficiency increased with increasing body mass in bumblebees and euglossine bees (Fig. 6A). Overall efficiency calculated assuming zero elastic energy storage was higher than that calculated assuming perfect elastic energy storage in bumblebees and euglossine bees for the original calculations; however, there was no significant difference in the slopes of the scaling relationships for overall efficiency calculated assuming zero and perfect elastic energy storage with body mass, for either group of bees. The revised calculations of profile power yielded higher mechanical power outputs than the previously published values (Casey and Ellington, 1989; Cooper, 1993). As a result of the increase in the estimate of mechanical power, the revised estimates of overall efficiency were significantly higher than those determined using the original calculations; overall efficiency similarly increased with increasing body mass for both bumblebees and euglossine bees (Fig. 6B). The difference between overall efficiency calculated assuming zero and perfect elastic energy storage was lower (though significantly different; P<0.001 for both bumblebees and euglossine bees) for the revised calculations compared with the original calculations (Fig. 6A,B). For bumblebees, the slope of the scaling relationship of overall efficiency and body mass was not significantly different between the original and revised calculations, assuming either zero (P>0.2) or perfect elastic energy storage (P>0.2), however, the intercepts of the relationships were significantly different (for zero elastic energy storage P<0.001; for perfect elastic energy storage P<0.001). For euglossine bees the slope of the scaling relationship of overall efficiency and body mass was not significantly different between the original and revised calculations assuming either zero

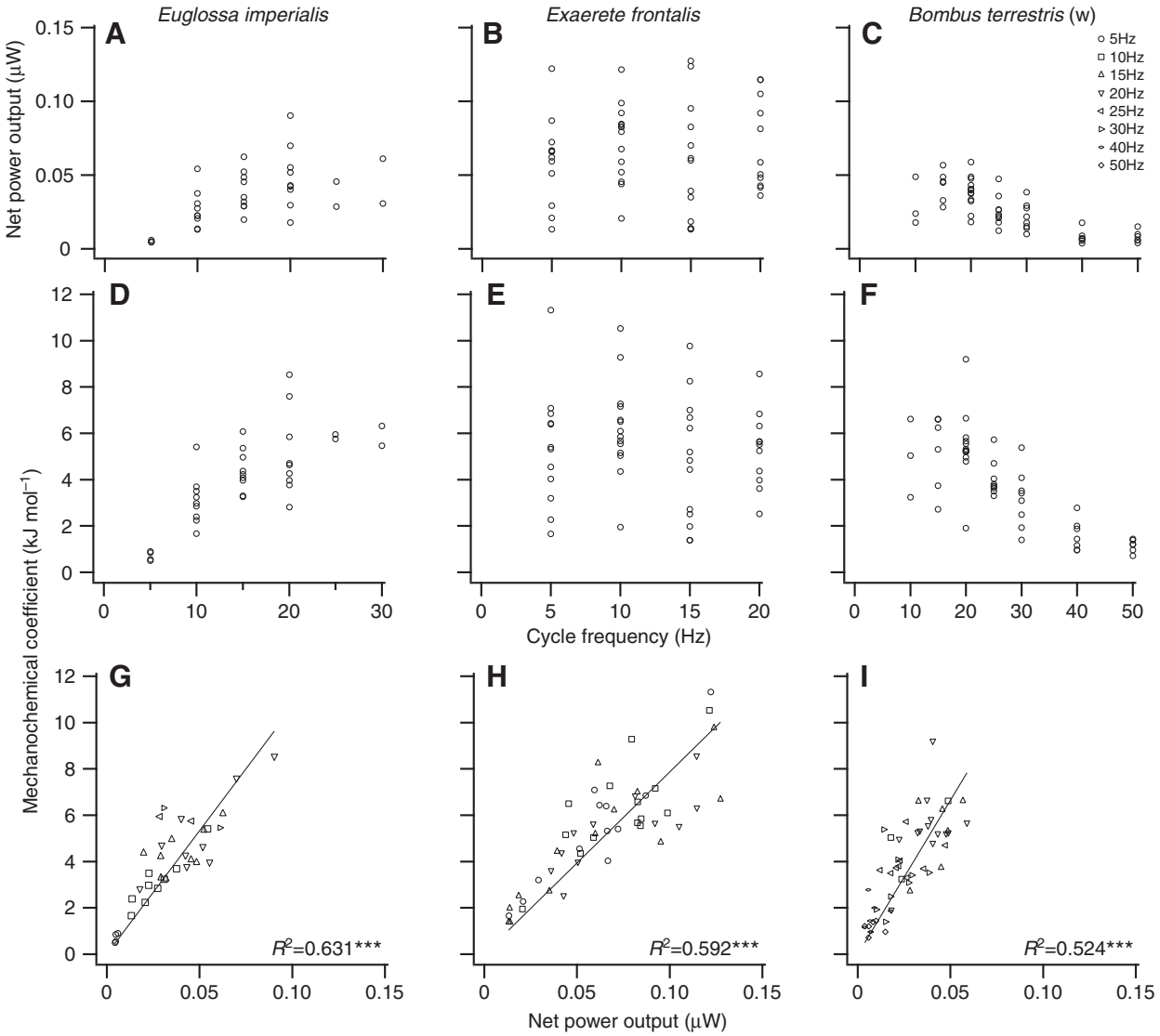

Fig. 4. The effect of cycle frequency on net power output (A–C) and mechanochemical coefficient (D–F) in glycerinated, asynchronous bee flight muscle fibres from (A,D) *Euglossa imperialis*, (B,E) *Exaerete frontalis* and (C,F) *Bombus terrestris* (worker). The highest mechanochemical coefficients were measured at cycle frequencies that were close to optimal for power generation. (G–I) The correlation between the mechanochemical coefficient and net power output for the same fibres plotted in A–F (different symbols denote the different cycle frequencies used in the experiments). Muscles that generated high mechanical power outputs also had higher mechanochemical coefficients. Statistically significant relationships are denoted by *** (P<0.002).

(P>0.2) or perfect elastic energy storage (P>0.2), however, the intercepts of the relationships were significantly different (for zero elastic energy storage P<0.001; for perfect elastic energy storage P<0.001). The slopes of the regression equations for the revised and original overall efficiency estimates and body mass were not significantly different for either bumblebees or euglossine bees (P>0.5 for both groups). The original observation that larger animals use less metabolic power to perform the same amount of mechanical power output as smaller species, giving an increase in overall efficiency of locomotion with increasing size, is upheld (Fig. 6).

DISCUSSION

Scaling of myofibrillar efficiency

This work represents the first attempt to study the influence of body mass on the myofibrillar efficiency in fibres performing oscillatory work. The main conclusion is that fibres from larger insects have a higher myofibrillar efficiency compared with those from smaller species. This is true for bumblebees and euglossine bees and for both apparent and gross efficiency calculations (Fig. 5A). Wingbeat frequency increases with decreasing body mass, resulting in a decrease in myofibrillar efficiency with increasing wingbeat frequency (Fig. 5B).

It has previously been proposed that faster muscles must activate and deactivate rapidly, requiring a greater overhead for the machinery of excitation–contraction coupling: a well developed sarcoplasmic reticulum, a high density of calcium release channels, a short diffusion pathway for calcium to the myofibrils (for rapid activation), a high density of SR calcium pumps, troponin with a low affinity for calcium, and high concentrations of parvalbumin [for rapid relaxation in some muscles (Tikunov and Rome, 2009)]. The lower efficiency of fast muscles might be due to the greater costs associated with processes such as the active uptake of calcium back into the SR, which liberate energy during contraction but yield no mechanical work (Curtin and Woledge, 1979; Curtin and

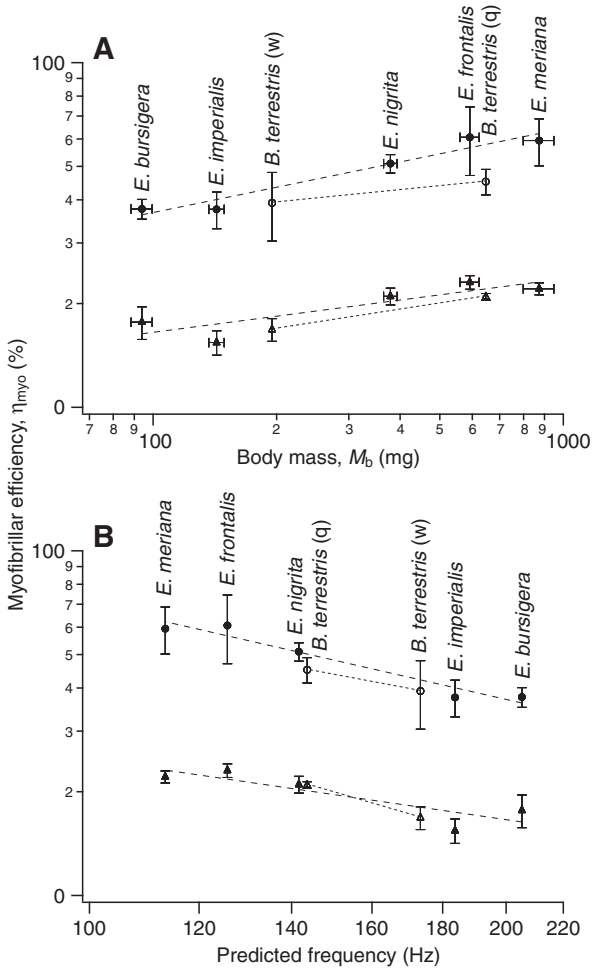

Fig. 5. Scaling of myofibrillar efficiency with (A) body mass and (B) wingbeat frequency in euglossine bees (filled symbols) and bumblebees (open symbols). Dashed lines are regressions for the euglossine bee data and dotted lines for the bumblebee data. Wingbeat frequency was calculated from body mass using scaling equations [bumblebees (Cooper, 1993); euglossine bees (Casey and Ellington, 1989)]. Both gross (triangles) and apparent (circles) myofibrillar efficiency are plotted in A,B. Scaling equations are reported for apparent myofibrillar efficiency ($\eta_{myo,\,app}$) and gross myofibrillar efficiency($\eta_{myo,\,gr}$) in Table 1. All relationships are statistically significant from zero (P<0.01).

Woledge, 1993a; Barclay, 1994). However, if these costs increase in proportion to the increase in power associated with the higher shortening velocities, efficiency should not be affected. In fast-twitch muscles calcium cycling contributes approximately one-third of the total energy costs during isometric contractions (Barclay et al., 2008), however, in the asynchronous muscles used in this study, calcium does not have to be released and absorbed with each contraction and calcium cycling costs are likely to be negligible (Josephson et al., 2000a). There must be additional reasons for the scaling of muscle efficiency than scaling of activation costs.

A crossbridge will do the most net-work if it attaches at its maximum extension and stays attached until its free energy is at a minimum [see figure 1D in Barclay (Barclay, 1994)]. Inefficiencies could arise by reducing the net work performed by the crossbridge (Woledge, 1968; Barclay, 1994): (1) the crossbridge could detach early, before completing a full work cycle; (2) the crossbridge could stay attached beyond the free minimum, resulting in absorption of work; or (3) the crossbridge could attach at a smaller extension than the maximum possible. Barclay (Barclay, 1994) used a two-state model of crossbridge kinetics to try to establish whether such a model can predict the different steady-state energetics of fast and slow muscles. His model predicts that in fast muscle, the relatively low rate of detachment of positively strained crossbridges results in more crossbridges remaining attached until they are strained negatively, thus opposing filament sliding and reducing net crossbridge work, compared with slow muscle. A further suggestion is that the more curved force–velocity relationship in slow compared with fast muscle results from the rapid decrease in the number of attached crossbridges as relative shortening velocity increases. If there are fewer crossbridges attached, it might increase the likelihood of a detached bridge finding a binding site in an optimal location, i.e. at full extension (Barclay, 1994). Faster contracting muscles from smaller insects may have lower myofibrillar efficiencies than those from slower muscles from larger insects for similar reasons.

Scaling of muscle mass-specific power for hovering and overall efficiency

Compared with the ‘original’ [following Ellington (Ellington, 1984)] approach to estimate mechanical power, the ‘revised’ estimates of $C_{D,pro}$ [following Ellington (Ellington, 1999)] resulted in an increase in the profile power. As a result, the total mechanical power requirements of hovering and therefore the overall locomotor efficiency were higher for the revised than the original calculations (Table 2, Fig. 6). The mechanical power required to overcome the drag associated with the LEV is substantial. The magnitude of the increase in mechanical power due to LEV drag depends on body mass and assumptions about whether there is zero or perfect elastic energy storage, but the increase in the total muscle mass-specific mechanical power over the original calculations ranges from a 2.2-fold for bumblebees and 2.2- to 2.6-fold for euglossine bees (perfect

Table 1. Gross and apparent myofibrillar efficiency of glycerinated dorsolongitudinal flight muscle from bumblebees and euglossine bees

	Bumblebees	Euglossine bees
Gross myofibrillar efficiency	$\eta_{myo,gr,bom}=6.4\ M_b^{0.18\pm0.04}$ $\eta_{myo,gr,bom}=6933\ n^{-1.17\pm0.14}$	$\eta_{myo,gr,eug}=8.1\ M_b^{0.16\pm0.03}$ $\eta_{myo,gr,eug}=365.1\ n^{-0.58\pm0.13}$
Apparent myofibrillar efficiency	$\eta_{myo,app,bom}=21.0\ M_b^{0.12\pm0.03}$ $\eta_{myo,app,bom}=1912\ n^{-0.75\pm0.09}$	$\eta_{myo,app,eug}=11.9\ M_b^{0.24\pm0.02}$ $\eta_{myo,app,eug}=4744\ n^{-0.92\pm0.09}$

Scaling equations of myofibrillar efficiency (η_{myo}) with body mass (M_b) and wing beat frequency (n) are given for euglossine bees and bumblebees (relationships illustrated in Fig. 5).

eug and bom (subscript), euglossine bee and bumblebee data sets, respectively; gr and app (subscript), gross and apparent myofibrillar efficiency, respectively.

In the scaling equations M_b is in mg, wing beat frequency is in Hz, η_{myo} is calculated as a percentage. Scaling exponents are presented ±95% confidence interval.

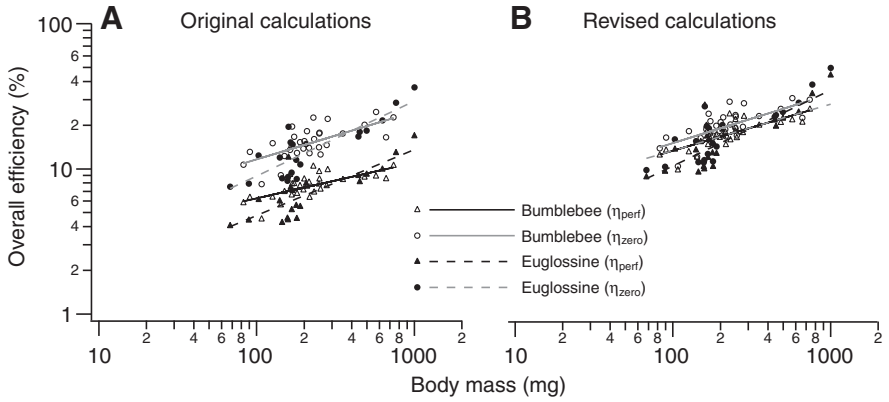

Fig. 6. Scaling of overall hovering efficiency and body mass. Overall efficiency was calculated as the ratio of mechanical to metabolic power determined using morphological, kinematic and metabolic data collected in previous studies for bumblebees [open symbols (Cooper, 1993)] and euglossine bees [filled symbols (Casey and Ellington, 1989)]. Mechanical power was estimated using either (A) 'original' calculations, in which the profile drag coefficient ($C_{D,pro}$) was calculated as $C_{D,pro}=7/\sqrt{Re}$ (following Ellington, 1984); or (B) 'revised' calculations, in which it was assumed that the lift to profile drag ratio was 1.7 (from Ellington, 1999). The scaling relationships of overall efficiency with body mass for the original and revised calculations are given in Table 2.

elastic energy storage) to a 1.3-fold for bumblebees and 1.3- to 1.4-fold for euglossine bees (zero elastic energy storage). Overall efficiency increased by a similar magnitude as the increase in mechanical power: 2.1- to 2.2-fold for bumblebees and 2.2-fold for euglossine bees (perfect elastic energy storage) to a 1.3-fold for bumblebees and 1.3-fold for euglossine bees (zero elastic energy storage). Because of the high sensitivity of the calculation of mechanical power to the value assumed for $C_{D,pro}$, and the uncertainty of assigning a value for $C_{D,pro}$, the magnitude of the revised estimates of overall efficiency should be treated cautiously. However, qualitatively the relationship between mechanical power (and therefore overall efficiency) and body mass (or wing beat frequency) is much less affected by the approach used to calculate mechanical power and is likely to be more robust (Table 2, Fig. 6).

Comparison between the scaling of myofibrillar and overall efficiency

The broad aim of this study was to establish the extent to which the scaling of overall efficiency with body mass is determined by the scaling of myofibrillar efficiency and, thereby indirectly, the scaling of mitochondrial oxidative recovery. Qualitatively, the increase in overall efficiency with body mass in both bumblebees and euglossine bees agrees with the increase in myofibrillar efficiency with body mass. However, the scaling exponent of the relationship between myofibrillar efficiency and body mass is lower than the scaling exponent of the relationship between overall efficiency and body mass (Fig. 5, Tables 1 and 2), indicating that the scaling of myofibrillar efficiency may not be the only determinant of the observed scaling of overall efficiency with body mass. The scaling exponent of myofibrillar efficiency with body mass ($\propto M_b^{0.16}$ or $M_b^{0.24}$ depending on whether gross of apparent efficiency is calculated and which group of bees is considered; Fig. 5, Table 1) is lower than that for the scaling of overall efficiency ($\propto M_b^{0.33}$ or $M_b^{0.53}$ depending on whether zero or perfect elastic energy storage is assumed and which group of bees is considered for the revised estimates of mechanical power; Table 2). Although the difference between the scaling exponents is not statistically significant ($P>0.2$ for both groups of bees regardless of the calculation method for either overall efficiency or myofibrillar efficiency), it can tentatively be concluded that the efficiency of mitochondrial oxidative recovery may also scale with body mass and wing beat frequency (increasing with increasing body mass and

Table 2. Mechanical and metabolic power requirements and overall efficiency of flight in bumblebees and euglossine bees

	Original calculations (following Ellington,1984)		Revised calculations (following Ellington, 1999)	
	Bumblebees	Euglossine bees	Bumblebees	Euglossine bees
Mechanical power output (zero elastic energy storage)	$P^*_{o,zero}=24\ M_b^{0.16\pm0.11}$ $P^*_{o,zero}=277\ n^{-0.31\pm0.51}$	$P^*_{o,zero}=33\ M_b^{0.10\pm0.05}$ $P^*_{o,zero}=134\ n^{-0.18\pm0.22}$	$P^*_{o,zero}=30\ M_b^{0.17\pm0.09}$ $P^*_{o,zero}=392\ n^{-0.32\pm0.44}$	$P^*_{o,zero}=41\ M_b^{0.11\pm0.05}$ $P^*_{o,zero}=217\ n^{-0.21\pm0.20}$
Mechanical power output (perfect elastic energy storage)	$P^*_{o,perf}=20\ M_b^{0.07\pm0.04}$ $P^*_{o,perf}=25\ n^{0.03\pm0.20}$	$P^*_{o,perf}=24\ M_b^{0.03\pm0.03}$ $P^*_{o,perf}=25\ n^{0.02\pm0.12}$	$P^*_{o,perf}=30\ M_b^{0.15\pm0.04}$ $P^*_{o,perf}=182\ n^{-0.20\pm0.27}$	$P^*_{o,perf}=38\ M_b^{0.10\pm0.04}$ $P^*_{o,perf}=162\ n^{-0.18\pm0.18}$
Metabolic power input	$P^*_i=997\ M_b^{-0.18\pm0.12}$ $P^*_i=3.2\ n^{0.94\pm0.41}$	$P^*_i=4.0\times10^3\ M_b^{-0.42\pm0.16}$ $P^*_i=0.58\ n^{1.29\pm0.56}$	$P^*_i=997\ M_b^{-0.18\pm0.12}$ $P^*_i=3.2\ n^{0.94\pm0.41}$	$P^*_i=3.9\times10^3\ M_b^{-0.42\pm0.16}$ $P^*_i=0.58\ n^{1.29\pm0.56}$
Overall efficiency (zero elastic energy storage)	$\eta_{zero}=2.4\ M_b^{0.34\pm0.14}$ $\eta_{zero}=8.8\times10^3\ n^{-1.24\pm0.62}$	$\eta_{zero}=0.83\ M_b^{0.52\pm0.15}$ $\eta_{zero}=2.3\times10^4\ n^{-1.46\pm0.64}$	$\eta_{zero}=3.1\ M_b^{0.35\pm0.13}$ $\eta_{zero}=1.2\times10^4\ n^{-1.26\pm0.58}$	$\eta_{zero}=1.0\ M_b^{0.53\pm0.16}$ $\eta_{zero}=3.7\times10^4\ n^{-1.50\pm0.65}$
Overall efficiency (perfect elastic energy storage)	$\eta_{perf}=2.0\ M_b^{0.25\pm0.10}$ $\eta_{perf}=783\ n^{-0.91\pm0.45}$	$\eta_{perf}=0.59\ M_b^{0.45\pm0.16}$ $\eta_{perf}=4.4\times10^3\ n^{-1.27\pm0.63}$	$\eta_{perf}=3.0\ M_b^{0.33\pm0.10}$ $\eta_{perf}=5.8\times10^3\ n^{-1.13\pm0.50}$	$\eta_{perf}=0.96\ M_b^{0.52\pm0.16}$ $\eta_{perf}=2.8\times10^4\ n^{-1.46\pm0.67}$

Scaling equations of body mass-specific power (P^*_m) and overall hovering efficiency (η) with body mass (M_b) and wing beat frequency (n) are given for euglossine bees (Casey and Ellington, 1989) and bumblebees (Cooper, 1993). The calculations of body mass-specific mechanical power output use kinematic and morphological data collected in previous investigations (Casey and Ellington, 1989; Cooper, 1993). To estimate the body mass-specific mechanical power requirements of hovering an aerodynamic analysis was carried out following Ellington (Ellington, 1984). For the 'original' calculations the profile drag coefficient ($C_{D,pro}$)was calculated as $C_{D,pro}=7/\sqrt{Re}$ (following Ellington, 1984). For the 'revised' calculations of mechanical power it was assumed that the lift to profile drag ratio was 1.7 (following Ellington, 1999). Body mass-specific metabolic power is given for both euglossine bees and bumblebees collected in previous investigations (Casey and Ellington, 1989; Cooper, 1993). Note that in the scaling equations M_b is in mg, wing beat frequency is in Hz, P^*_o is calculated in W kg^{-1} body mass and η is calculated as %. Scaling exponents are presented ±95% confidence interval.

decreasing with increasing wing beat frequency. This is considered in more detail below.

The magnitude of the myofibrillar efficiency depends on whether the apparent or gross myofibrillar efficiency is considered. For bumblebees, apparent myofibrillar efficiency was 2.2 to 2.4 times greater than the gross myofibrillar efficiency; for euglossine bees, apparent myofibrillar efficiency was 2.1 to 2.5 times greater than the gross myofibrillar efficiency. In the following sections comparisons are made between the overall efficiency determined using the revised calculations and the gross or apparent myofibrillar efficiency.

For a given body mass, the revised overall efficiency (calculated assuming either zero or perfect elastic energy storage) was similar to the gross myofibrillar efficiency. It is surprising to find that the overall efficiency is similar to the gross myofibrillar efficiency. The overall efficiency is determined by the product of the efficiencies of the constituent processes (e.g. myofibrillar and mitochondrial oxidative recovery efficiencies); the myofibrillar efficiency being only one component of the overall efficiency should therefore be larger than overall efficiency. In fact it should be approximately twice as large as the overall efficiency if it is assumed that the efficiency of mitochondrial oxidative recovery (the main additional component of the overall efficiency) is approximately 50% (Hinkle et al., 1991). Based on the scaling exponents for overall [revised estimates calculated following Ellington (Ellington, 1999)] and gross myofibrillar efficiency, the efficiency of mitochondrial oxidative recovery (η_{mito}) is predicted to increase with increasing body mass, scaling as $\eta_{mito,\,zero} \propto n^{-0.09} \propto M_b^{0.17}$ and $\eta_{mito,\,perf} \propto n^{0.04} \propto M_b^{0.15}$ in bumblebees and as $\eta_{mito,\,zero} \propto n^{-0.92} \propto M_b^{0.38}$ and $\eta_{mito,\,perf} \propto n^{-0.88} \propto M_b^{0.37}$ in euglossine bees. In bumblebees the overall efficiency for both zero and perfect elastic energy storage exceeds the gross myofibrillar efficiency, giving the prediction that the mitochondrial oxidative recovery efficiency exceeds 100%. It is also the case in large euglossine bees that η_{mito} is predicted to exceed 100% where the gross myofibrillar efficiency has been compared with overall efficiency estimates calculated assuming either perfect or elastic energy storage. Clearly this is unrealistic and suggests that either the mechanical power (and hence overall efficiency) has been over-estimated, or that the gross myofibrillar efficiency has been under-estimated. However, the possible scaling of mitochondrial oxidative recovery efficiency with body mass is a new and interesting observation.

Based on the scaling exponents for revised overall and apparent myofibrillar efficiency, the mitochondrial oxidative recovery efficiency (η_{mito}) is predicted to increase with increasing body mass and decreasing muscle operating frequency, scaling as $\eta_{mito,\,zero} \propto n^{-0.51} \propto M_b^{0.23}$ and $\eta_{mito,\,perf} \propto n^{-0.38} \propto M_b^{0.21}$ in bumblebees and as $\eta_{mito,\,zero} \propto n^{-0.58} \propto M_b^{0.29}$ and $\eta_{mito,\,perf} \propto n^{-0.54} \propto M_b^{0.28}$ in euglossine bees. Assuming zero elastic energy storage, this gives a mitochondrial oxidative recovery efficiency range of 50–66% in bumblebees and 31–60% in euglossine bees. Assuming perfect elastic energy storage, mitochondrial oxidative recovery efficiency ranges from 44 to 56% in bumblebees and 29 to 54% in euglossine bees. These values are similar to those expected (Hinkle et al., 1991). However, it is unlikely that the apparent efficiency is appropriate for comparison with the overall hovering efficiency; it is the gross efficiency that should be considered. The rationale for the approach to calculate apparent efficiency is unclear as it seems unlikely that any of the crossbridges can have the same function in isometric and cyclically contracting muscle. The approach may over-estimate the MC by ignoring the ATP used by some of the crossbridges that contribute to the generation of work.

Comparison with myofibrillar efficiency in other insects with asynchronous muscles

The efficiency of asynchronous flight muscle from the giant waterbug *Lethocerus* has been determined using a number of different techniques. MCs of 7.9 kJ mol^{-1} [range 4 to 16 kJ mol^{-1} (Rüegg and Tregear, 1966)], 10.7 kJ mol^{-1} [when the regression in their figure 3 is constrained to go through zero (Pybus and Tregear, 1975)] and 11.7 kJ mol^{-1} (G.N.A., R.T.T. and C.P.E., unpublished observations) have been measured. These values are similar or slightly higher than the highest MCs measured for the largest bees in these experiments (8.8–9.7 kJ mol^{-1}). However, it should be noted that the mass of *Lethocerus* used in these experiments is approximately 10 g, and it might therefore be expected to have quite a high myofibrillar efficiency given the positive scaling of myofibrillar efficiency with body mass (Table 2, Fig. 5A).

The overall efficiency of the flight muscle of a beetle, estimated using respirometry and the work loop technique, at a cycle frequency equivalent to its wingbeat frequency, was 11–12% (Josephson et al., 2000b). The wingbeat frequency of this species of beetle is slightly lower than the lowest predicted wingbeat frequency of the bees used in our experiments (90 Hz in the beetle compared with 100 Hz in the largest euglossine bee). We cannot be certain whether the scaling equations determined for wingbeat frequencies of 100–200 Hz hold down to this lower frequency, or whether the scaling equations for apid bees are applicable to other orders of insects with asynchronous flight muscles. However, if these uncertainties are ignored, the gross myofibrillar efficiency at a wingbeat frequency of 90 Hz is predicted to be 26%. Assuming a mitochondrial oxidative recovery efficiency of 51% (Hinkle et al., 1991), an overall efficiency of 13% would be predicted. Despite the uncertainties it may not be unreasonable to assume that it is not completely fortuitous that the predicted and measured overall efficiencies are so similar.

Considerations in assessing the reliability of the measurements of myofibrillar efficiency

There are a number of factors that must be contemplated when making comparisons between the myofibrillar and overall efficiencies. First, the mechanical performance of skinned fibres differs from that expected. Maximum power output was obtained at a lower cycle frequency than the wingbeat frequency predicted from scaling equations. In addition, the optimum cycle frequency for bumblebee fibres was also lower than that previously measured at a similar temperature (Gilmour and Ellington, 1993). However, it should be noted that in this earlier work, power output was measured using a constant strain of 0.01, which will yield a higher optimum cycle frequency than our experiments in which strain was optimised at each cycle frequency. Their experiments showed that the optimum cycle frequency increased with increasing temperature. This explains part of the discrepancy between optimum frequency *in vitro* and wingbeat frequency, but even at a temperature of 40°C [close to the thoracic temperature during flight (Heinrich, 2004; Joos et al., 1991)] the operating frequency was approximately half the *in vivo* wingbeat frequency. It was proposed that subtle differences in the composition of the incubation medium used *in vitro* and the intracellular environment of the muscle fibres might result in such a frequency discrepancy (Gilmour and Ellington, 1993). Similar effects may have resulted

in the optimum frequency in our *in vitro* experiments being lower than the wingbeat frequency *in vivo*, but whether this would have any effect on muscle efficiency is unknown.

Second, as noted above, the temperature at which the experiments were conducted was lower than the thoracic temperature of bees during flight (Heinrich, 2004; Joos et al., 1991). There is some evidence that temperature has little effect on efficiency (e.g. Gibbs and Chapman, 1974; Rall and Woledge, 1990), however, it has also been reported that myofibrillar efficiency during isotonic shortening contractions increased with increasing temperature (He et al., 2000). Thus the effect that the lower experimental temperature might have on myofibrillar efficiency are inconclusive.

Third, it has been suggested that inadequate diffusion of ATP in and ADP out of the myofibril may limit the performance of glycerinated muscle fibre preparations (Josephson et al., 2000b). When the supply of ATP by diffusion is insufficient to meet that being used by the fibre, glycerinated fibres enter what has been termed the 'high tension state'. In the high tension state, positive work can only be sustained for a small number of cycles after which the mean force developed by the fibre increases and the work declines (Steiger and Rüegg, 1969). The majority of fibres in our experiments maintained a constant level of work during the oscillations, indicating that the fibres used in these experiments were not diffusion limited. Occasionally, the work output of the muscle declined during the period of oscillation, but this could usually be recovered by stretching the muscle slightly. In cases where work did not recover during cycling, the mean force did not increase and poor performance was probably caused by damage during the dissection or paring of the fibre rather than it entering a high tension state. Results from such preparations were excluded from our analysis.

Fourth, the free energy of ATP hydrolysis (ΔG_{ATP}) may differ between the intracellular conditions provided for the skinned muscle preparations and whole muscles (Smith et al., 2005).

Concluding remarks

In conclusion, we have shown increases in the efficiency with which the myofibrils convert the chemical energy in ATP into net mechanical work with increasing body mass. With the reduction in wingbeat frequency with increasing body mass, this supports the hypothesis that faster cycling muscles from different species are less efficient than muscles operating at lower cycle frequencies. The scaling exponent for the variation of myofibrillar efficiency with body mass is lower but not significantly different from the exponent for the scaling of overall efficiency with mass. This suggests that the efficiency of mitochondrial oxidative recovery may also scale with body mass. The finding that the myofibrillar efficiency was similar to the overall hovering efficiency was surprising, and we are currently unable to explain this anomaly.

ACKNOWLEDGEMENTS

This work was supported by the BBSRC (grant S10245 to C.P.E. and Prof. J. D. Altringham, University of Leeds). We are grateful to the Smithsonian Tropical Research Institute for supporting our work at Barro Colorado Island. We would like to thank Mike Reedy for sharing with us his techniques for the glycerination of insect flight muscle.

REFERENCES

Alexander, R. M. (2005). Models and the scaling of energy costs for locomotion. *J. Exp. Biol.* **208**, 1645-1652.

Altringham, J. D. and Johnston, I. A. (1990). Modeling muscle power output in a swimming fish. *J. Exp. Biol.* **148**, 395-402.

Askew, G. N. and Marsh, R. L. (1997). The effects of length trajectory on the mechanical power output of mouse skeletal muscles. *J. Exp. Biol.* **200,** 3119-3131.

Barclay, C. J. (1994). Efficiency of fast-twitch and slow-twitch muscles of the mouse performing cyclic contractions. *J. Exp. Biol.* **193**, 65-78.

Barclay, C. J. (1996). Mechanical efficiency and fatigue of fast and slow muscles of the mouse. *J. Physiol.* **497**, 781-794.

Barclay, C. J. (1998). Estimation of cross-bridge stiffness from maximum thermodynamic efficiency. *J. Muscle Res. Cell Motil.* **19**, 855-864.

Barclay, C. J. and Weber, C. L. (2004). Slow skeletal muscles of the mouse have greater initial efficiency than fast muscles but the same net efficiency. *J. Physiol.* **559**, 519-533.

Barclay, C. J., Constable, J. K. and Gibbs, C. L. (1993). Energetics of fast-twitch and slow-twitch muscles of the mouse. *J. Physiol.* **472**, 61-80.

Barclay, C. J., Lichtwark, G. A. and Curtin, N. A. (2008). The energetic cost of activation in mouse fast-twitch muscle is the same whether measured using reduced filament overlap or N-benzyl-p-toluenesulphonamide. *Acta Physiol.* **193**, 381-391.

Borrell, B. J. and Medeiros, M. J. (2004). Thermal stability and muscle efficiency in hovering orchid bees (Apidae: Euglossini). *J. Exp. Biol.* **207**, 2925-2933.

Buschman, H. P. J., Elzinga, G. and Woledge, R. C. (1996). The effects of the level of activation and shortening velocity on energy output in type 3 muscle fibres from *Xenopus laevis*. *Pflugers Archiv.* **433**, 153-159.

Buschman, H. P. J., Linari, M., Elzinga, G. and Woledge, R. C. (1997). Mechanical and energy characteristics during shortening in isolated type-1 muscle fibres from *Xenopus laevis* studied at maximal and submaximal activation. *Pflugers Archiv.* **435**, 145-150.

Casey, T. M. and Ellington, C. P. (1989). Energetics of insect flight. In *Energy Transformation in Cells and Organisms* (ed. W. Wieser and E. Gnaiger), pp. 200-210. Stuttgart: Georg Thieme Verlag.

Cooper, A. J. (1993). Limitations of bumblebee flight performance. PhD thesis, University of Cambridge, Cambridge.

Curtin, N. A. and Woledge, R. C. (1979). Chemical change and energy production during contraction of frog muscle. How are their time courses related? *J. Physiol.* **288**, 353-366.

Curtin, N. A. and Woledge, R. C. (1993a). Efficiency of energy conversion during sinusoidal movement of red muscle fibres from the dogfish *Scyliorhinus canicula*. *J. Exp. Biol.* **185**, 195-206.

Curtin, N. A. and Woledge, R. C. (1993b). Efficiency of energy conversion during sinusoidal movement of white muscle fibres from the dogfish *Scyliorhinus canicula*. *J. Exp. Biol.* **183**, 137-147.

Darveau, C. A., Hochachka, P. W., Roubik, D. W. and Suarez, R. K. (2005). Allometric scaling of flight energetics in orchid bees: evolution of flux capacities and flux rates. *J. Exp. Biol.* **208**, 3593-3602.

Dickinson, M. H. and Lighton, J. R. B. (1995). Muscle efficiency and elastic storage in the flight motor of Drosophila. *Science* **268**, 87-90.

Ellerby, D. J., Henry, H. T., Carr, J. A., Buchanan, C. I. and Marsh, R. L. (2005). Blood flow in guinea fowl Numida meleagris as an indicator of energy expenditure by individual muscles during walking and running. *J. Physiol.* **564**, 631-648.

Ellington, C. P. (1984). The aerodynamics of hovering insect flight. VI. Lift and power requirements. *Phil. Trans. R. Soc. London Ser. B* **305**, 145-181.

Ellington, C. P. (1999). The novel aerodynamics of insect flight: applications to micro-air vehicles. *J. Exp. Biol.* **202**, 3439-3448.

Ellington, C. P., vandenBerg, C., Willmott, A. P. and Thomas A. L. R. (1996). Leading-edge vortices in insect flight. *Nature* **384**, 626-630.

Gibbs, C. L. and Chapman, J. B. (1974). Effects of stimulus conditions, temperature, and length on energy output of frog and toad sartorius. *Am. J. Physiol.* **227**, 964-971.

Gilmour, K. M. and Ellington, C. P. (1993). Power output of glycerinated bumblebee flight muscle. *J. Exp. Biol.* **183**, 77-100.

Glyn, H. and Sleep, J. (1985). Dependence of adenosine triphosphatase activity of rabbit psoas muscle fibres and myofibrils on substrate concentration. *J. Physiol.* **365**, 259-276.

He, Z. H., Bottinelli, R., Pellegrino, M. A., Ferenczi, M. A. and Reggiani, C. (2000). ATP consumption and efficiency of human single muscle fibers with different myosin isoform composition. *Biophys. J.* **79**, 945-961.

Heinrich, B. (2004). *Bumblebee Economics.* Cambridge, MA: Harvard University Press.

Hinkle, P. C., Kumar, M. A., Resetar, A. and Harris, D. L. (1991). Mechanistic stoichiometry of mitochondrial oxidative phosphorylation. *Biochemistry* **30**, 3576-3582.

Jewell, B. R. and Rüegg, J. C. (1966). Oscillatory contraction of insect fibrillar muscle after glycerol extraction. *Proc. R. Soc. London B Biol. Sci.* **164**, 428-459.

Joos, B., Young, P. A. and Casey, T. M. (1991). Wingstroke frequency of foraging and hovering bumblebees in relation to morphology and temperature. *Physiol. Entomol.* **16**, 191-200.

Josephson, R. K. (1985). Mechanical power output from striated muscle during cyclic contraction. *J. Exp. Biol.* **114**, 493-512.

Josephson, R. K. (1997). Power output from a flight muscle of the bumblebee *Bombus terrestris*. 3. Power during simulated flight. *J. Exp. Biol.* **200**, 1241-1246.

Josephson, R. K., Malamud, J. G. and Stokes, D. R. (2000a). Asynchronous muscle: a primer. *J. Exp. Biol.* **203**, 2713-2722.

Josephson, R. K., Malamud, J. G. and Stokes, D. R. (2000b). Power output by an asynchronous flight muscle from a beetle. *J. Exp. Biol.* **203**, 2667-2689.

Josephson, R. K., Malamud, J. G. and Stokes, D. R. (2001). The efficiency of an asynchronous flight muscle from a beetle. *J. Exp. Biol.* **204**, 4125-4139.

Kushmerick, M. J. and Davies, R. E. (1969). The chemical energetics of muscle contraction II. The chemistry, efficiency and power of maximally working sartorius muscles. *Proc. R. Soc. Lond. B Biol. Sci.* **174**, 315-353.

Loxdale, H. D. (1976). Method for continuous assay of picomole quantities of ADP released from glycerol extracted skeletal muscle fibres on MgATP activation. *J. Physiol.* **260,** P4-P5.

Machin, K. E. and Pringle, J. W. S. (1959). The physiology of insect fibrillar muscle. 2. Mechanical properties of a beetle flight muscle. *Proc. R. Soc. Lond. B Biol. Sci.* **151**, 204-225.
Potma, E. J. and Stienen, G. J. M. (1996). Increase in ATP consumption during shortening in skinned fibres from rabbit psoas muscle: Effects of inorganic phosphate. *J. Physiol.* **496**, 1-12.
Pringle, J. W. S. and Tregear, R. T. (1969). Mechanical properties of insect fibrillar muscle at large amplitudes of oscillation. *Proc. R. Soc. Lond. B Biol. Sci.* **174**, 33-50.
Pybus, J. and Tregear, R. T. (1975). Relationship of adenosine triphosphatase activity to tension and power output of insect flight muscle. *J. Physiol.* **247**, 71-89.
Rall, J. A. and Woledge, R. C. (1990). Influence of temperature on mechanics and energetics of muscle contraction. *Am. J. Physiol.* **259**, R197-R203.
Reggiani, C., Potma, E. J., Bottinelli, R., Canepari, M., Pellegrino, M. A. and Stienen, G. J. M. (1997). Chemo-mechanical energy transduction in relation to myosin isoform composition in skeletal muscle fibres of the rat. *J. Physiol.* **502**, 449-460.
Rome, L. C. and Klimov, A. A. (2000). Superfast contractions without superfast energetics: ATP usage by SR-Ca^{2+} pumps and crossbridges in toadfish swimbladder muscle. *J. Physiol.* **526**, 279-286.
Roubik, D. W. and Ackerman, J. D. (1987). Long-term ecology of euglossine orchid-bees (Apidae, Euglossini) in Panama. *Oecologia* **73**, 321-333.
Rüegg, J. C. and Stumpf, H. (1969). Coupling of power output and myofibrillar ATPase activity in glycerol extracted insect fibrillar muscle at varying amplitude of ATP driven oscillation. *Pflugers Archiv.* **305**, 21-33.
Rüegg, J. C. and Tregear, R. T. (1966). Mechanical factors affecting ATPase activity of glycerol extracted insect fibrillar flight muscle. *Proc. R. Soc. Lond. B Biol. Sci.* **165**, 497-512.
Sane, S. P. and Dickinson, M. H. (2001). The control of flight force by a flapping wing: lift and drag production. *J. Exp. Biol.* **204**, 2607-2626.
Smith, N. P., Barclay, C. J. and Loiselle, D. S. (2005). The efficiency of muscle contraction. *Prog. Biophys. Mol. Biol.* **88**, 1-58.
Steiger, G. J. and Rüegg, J. C. (1969). Energetics and efficiency in isolated contractile machinery of an insect fibrillar muscle at various frequencies of oscillation. *Pflugers Archiv.* **307**, 1-21.
Stienen, G. J. M., Kiers, J. L., Bottinelli, R. and Reggiani, C. (1996). Myofibrillar ATPase activity in skinned human skeletal muscle fibres: Fibre type and temperature dependence. *J. Physiol.* **493**, 299-307.
Suarez, R. K., Darveau, C. A., Welch, K. C., O'Brien, D. M., Roubik, D. W. and Hochachka, P. W. (2005). Energy metabolism in orchid bee flight muscles: carbohydrate fuels all. *J. Exp. Biol.* **208**, 3573-3579.
Syme, D. A., Connaughton, M. A. and Rome, L. C. (1997). Apparatus for measuring steady-state ATP utilization rates of single muscle fibers. *Biol. Bull.* **193**, 251-253.
Tikunov, B. A. and Rome, L. C. (2009). Is high concentration of parvalbumin a requirement for superfast relaxation? *J. Muscle Res. Cell Motil.* **30**, 57-65.
Woledge, R. C. (1968). Energetics of tortoise muscle. *J. Physiol.* **197**, 685-707.
Zar, J. H. (1996). *Biostatistical Analysis.* London: Prentice-Hall International (UK) Ltd.